



LAWRENCE
LIVERMORE
NATIONAL
LABORATORY

UCRL-CONF-152425

Studies of Electron Transport and Isochoric Heating and Their Applicability to Fast Ignition

M. H. Key, F. Amiranoff, C. Andersen, D. Batani, S. D. Baton, T. Cowan, N. Fisch, R. Freeman, L. Gremillet, T. Hall, S. Hatchett, J. Hill, J. King, R. Kodama, J. Koch, M. Koenig, B. Lasinski, B. Landgon, A. MacKinnon, E. Martinolli, P. Norreys, P. Parks, E. Perelli-Cippo, M. Rabec Le Gloahec, M. Rosenbluth, C. Rousseaux, J. J. Santon, F. Scianitti, R. Snavely, M. Tabak, K. Tanaka, R. Town, T. Tsutumi, and R. Stephens

October 30, 2003

2003 Third International Conference on Inertial Fusion
Sciences and Applications, Monterey, California,
September 7-12, 2003

This document was prepared as an account of work sponsored by an agency of the United States Government. Neither the United States Government nor the University of California nor any of their employees, makes any warranty, express or implied, or assumes any legal liability or responsibility for the accuracy, completeness, or usefulness of any information, apparatus, product, or process disclosed, or represents that its use would not infringe privately owned rights. Reference herein to any specific commercial product, process, or service by trade name, trademark, manufacturer, or otherwise, does not necessarily constitute or imply its endorsement, recommendation, or favoring by the United States Government or the University of California. The views and opinions of authors expressed herein do not necessarily state or reflect those of the United States Government or the University of California, and shall not be used for advertising or product endorsement purposes.

Paper Number

STUDIES OF ELECTRON TRANSPORT AND ISOCHORIC HEATING AND THEIR APPLICABILITY TO FAST IGNITION

M. H. Key¹, F. Amiranoff⁵, C. Andersen², D. Batani⁷, S.D. Baton⁵, T. Cowan³, N. Fisch⁴, R. Freeman², L. Gremillet⁵, T. Hall⁸, S. Hatchett¹, J. Hill², J. King², R. Kodama¹⁰, J. Koch¹, M. Koenig⁵, B. Lasinski¹, B. Langdon¹, A. MacKinnon¹, E. Martinolli⁵, P. Norreys⁹, P. Parks³, E. Perelli-Cippo⁷, M. Rabec Le Gloahec⁶, M. Rosenbluth³, C. Rousseaux⁶, J.J. Santon⁵, F. Scianitti⁷, R. Snavely², M. Tabak, K. Tanaka¹⁰, R. Town, T. Tsutsumi¹⁰, R. Stephens³

¹Lawrence Livermore National Laboratory, Livermore, CA 94550, USA. Key1@llnl.gov

²Department of Applied Sciences, University of California, Davis, Davis, CA 95616, USA

³General Atomics, San Diego, CA, USA 92186, USA

⁴Princeton University, Princeton NJ, 08543SA

⁵Laboratoire pour l'Utilisation des Lasers Intenses, UMR 7605, CNRS-CEA-Universite Paris VI-Ecole Polytechnique, 91128 Palaiseau, France

⁶Commissariat a l'energie Atomique, 91680 Bruyeres-le-Chatel, France

⁷Dispartimento di Fisica G. Ochiolini, Universita degli Studi di Milano-Bicocca and INFN, Via Emanueli 15, 20126 Milan, Italy

⁸Department of Physics, University of Essex, Colchester CO4 3SQ, United Kingdom

⁹Rutherford Appleton Laboratory, Chilton, Oxon, OX110QX, United Kingdom

¹⁰Institute for Laser Engineering, Osaka University, Suita Osaka, Japan

Abstract

Experimental measurements of electron transport and isochoric heating in 100 J, 1 ps laser irradiation of solid Al targets are presented. Modeling with a hybrid PIC code is compared with the data and good agreement is obtained using a heuristic model for the electron injection. The relevance for fast ignition is discussed.

Introduction

The generation of relativistic electrons by intense laser radiation, their transport into dense matter and consequent effects (notably isochoric heating), are the central physical processes in a range of potentially important applications of PW class lasers. These applications include intense hard x-ray sources for pulsed radiography, isochoric heating for the study of high energy density matter, the generation and applications (in radiography, deflectometry, isochoric heating and production of radio-nuclides) of intense collimated beams of high energy protons and fast ignition of fusion by electrons or protons.

In an on going study ¹ of electron generation, transport and isochoric heating aimed particularly at providing a benchmarked numerical model suitable for scaled up design of applications such as fast ignition, we are seeking to reconcile experimental measurements with hybrid PIC modeling using adaptations of the LSP code².

Our experimental observations are principally on planar Al foil targets and include imaging of rear surface thermal XUV emission ($h\nu=68\text{eV}$) to obtain temperature patterns and measurement of transport

patterns and inferences of heating from the imaging of electron induced $K\alpha$ emission in buried layers of Cu. The data are from experiments conducted in collaborations at the 10J, 100fs JanUSP laser at LLNL, at the LULI laboratory in France with a 40TW, 0.5 ps laser, at the Vulcan laser facility in the UK with a 100TW, 1 ps laser and at the Petawatt beamline of the ILE Osaka Gekko laser facility in Japan with 200J, 1 ps pulses.

Experimental data

Data discussed here are those for 100J, 1 ps irradiation at the Vulcan laser with a peak intensity of $4\times 10^{19}\text{ Wcm}^{-2}$ in an intensity pattern with a central spot containing of 30% of the energy and broad quasi exponential wings. Imaging of Cu $K\alpha$ fluorescence from buried layers of Cu in Al targets shows a minimum spot diameter of about 70 μm for a 25 μm Cu foil target, significantly larger than the laser focal spot both in its central peak and its broad wings. The diameter increases in a 40° cone with increasing thickness of the Al transport layer in front of the Cu. Rear surface XUV images show a 70 to 100 μm wide central peak which decreases rapidly in intensity with increasing target thickness and disappears for thickness $>100\text{ }\mu\text{m}$. There is also a broad low intensity pediment about 800 μm wide, the intensity of which reduces only weakly with increasing target thickness.

The XUV images are dominated by near-Planckian thermal emission which for the measured 68 eV photon energy is very sensitive to temperature in the $kT=10$ to 100eV range of interest. The images

have been converted to absolute brightness using the counts per incident photon response of the CCD, the Al/polyimide filter transmission factors and the reflectivities of the XUV multi-layer mirrors. Radiation/hydro-dynamic modeling with Lasnex has been used to compute the integrated absolute brightness as a function of the initial temperature of the isochorically heated Al (see figure 1).

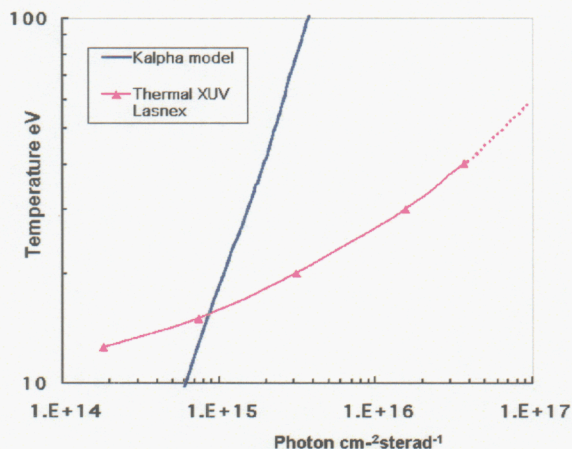


Figure 1 Temperature from absolute $K\alpha$ brightness and absolute XUV brightness

The images have thus been converted to maps of initial temperature. A line out through such an image in figure 2 exhibits a 70 μm (fwhm) 30 eV temperature peak and an 800 μm wide region at 10 to 15 eV. Reducing the target thickness to 40 μm increased the temperature peak to about 100eV.

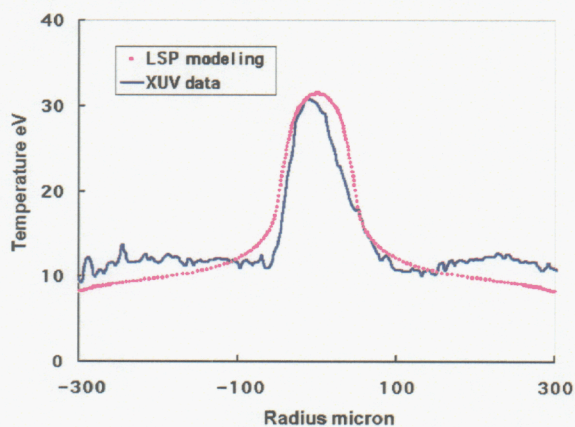


Figure 2 Rear surface temperature profile of a 100 μm thick Al target (XUV data) and computed profile from LSP.

In order to interpret the $K\alpha$ images as a measure of the isochoric heating we compute the collisional electron energy loss rate, the Ohmic heating and the rate of excitation of $K\alpha$. This was in a 1D approximation with all electrons in either a Maxwellian or Boltzmann distribution passing a reference plane in a 1ps pulse with a specified total energy and temperature. The resistivity was assumed to be $10^{-6}\Omega\text{m}$ at the plateau value for solid density Al which occurs in the range 10 to 100eV³. Temperature was obtained from energy density using the Sesame tabulations. For heating to 1GJ/kg (26eV) the required electron energy in 100 μm diameter varied almost linearly with hot electron temperature from 5J to 20 J in the range 300eV to 1200eV. For a Boltzmann distribution the energy range was slightly lower at 3.2 to 13.5 J. In all cases the collisional heating was a minor fraction of the total heating varying slowly from 21% to 33% for the extremes of 1200keV (Maxwellian) to 300keV (Boltzmann). The collisional fraction decreases with increasing heating, for example in the range 0.3 to 3 GJ/kg decreasing from 37% to 15%.

The fluorescent yield for a given amount of heating is rather insensitive to the electron temperature or form of the electron energy distribution function. For the $kT=26\text{ eV}$ example, the absolute yield of $K\alpha$ (evaluated for a thin layer and scaled to a 25 μm layer assuming no change in electron energy spectrum but allowing for re-absorption) for a Maxwellian or Boltzmann energy spectrum in the temperature range 300 to 1200keV varies only in the range 1.3 to 1.7×10^{15} photons $\text{cm}^{-2}\text{sterad}^{-1}$. The local $K\alpha$ brightness can therefore be related to the local temperature of the Al adjacent to the Cu layer. Figure 1 shows the brightness/temperature relationship for a 600keV Maxwellian. The deduced temperature changes by less than 10% if the assumed electron temperature is changed in the range 400 to 900keV.

The absolute $K\alpha$ image brightness was obtained by comparing the measured absolute $K\alpha$ yield from a 25 μm Cu foil (recorded by a CCD operated as single hit photon energy spectrometer), with the integrated signal in the corresponding $K\alpha$ image. In figure 3 compiled data show the peak temperature as a function of Al transport layer thickness deduced from the peak absolute $K\alpha$ brightness. The plot shows a sharp fall in heating with depth and while there is some random variation, the temperature at 100 μm depth agrees reasonably with that from the XUV data in figure 2

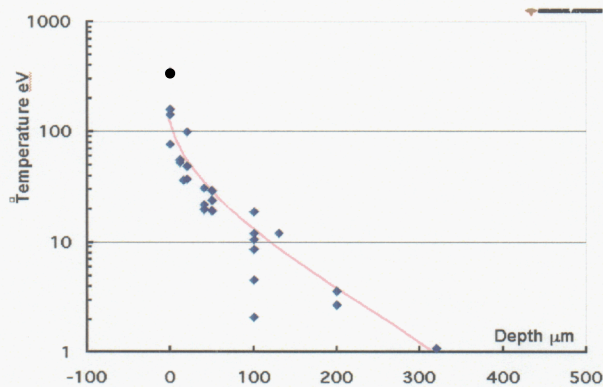


Figure 3 The peak temperature from absolute $K\alpha$ images as a function of depth in Al.

The same procedure enables transformation of $K\alpha$ images to temperature maps, e.g. in figure 4 at 100 μm depth showing a peak temperature and peak width in good agreement with the XUV data in figure 2. The broad low temperature pediment in the XUV data is not seen in the $K\alpha$ data. This difference is discussed later.

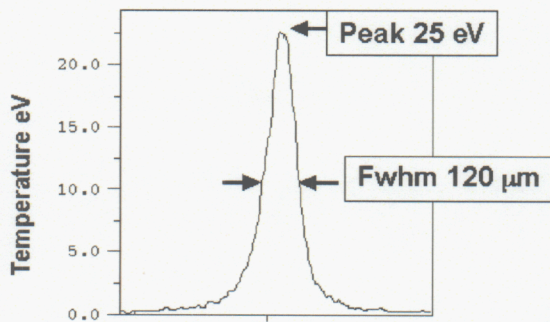


Figure 4 Temperature profile from the absolute $K\alpha$ image at 100 μm depth in an Al100/Cu25/Al20 μm target.

Modeling

Needed for the development of fast ignition and other applications is benchmarked integrated modeling capable of predicting the generation transport and deposition of energy by relativistic electrons. We have used hybrid PIC modeling with the LSP code to describe transport and heating in the dense part of the target⁴. The model was used 2D cylindrical coordinates. The Al target was represented as a fluid Al^{3+} plasma with ideal plasma properties. The Spitzer resistivity was clamped at 10^{-6}

Ohm m for all temperatures below that at which the limit is reached, in order to approximate the plateau in resistivity of solid density Al (This does not describe the fall to the metallic conductivity of 10^{-8} Ohm m at very low temperatures). The energy density in the fluid due to collisional and Ohmic electron heating was computed and temperatures were obtained by post processing using the Sesame equation of state tables.

The laser-generated electrons were treated by an implicit particle in cell method and were injected at the solid density surface of the target. An heuristic model was developed for their characteristics. Measured laser focal spot intensity patterns defined a radial profile of intensity and the local axial electron temperature was specified from the empirical scaling $kT/1\text{keV} = 100(I/10^{17} \text{ Wcm}^{-2})$ based on compiled experimental data. A constant transverse temperature of 200keV was assumed giving an increasingly diffuse electron source at lower energies in the wings of the focal spot. This transverse temperature choice was based on Monte-Carlo modeling which was most successful in fitting the cone angle of the experimental $K\alpha$ data with a similar prescription for the injected electrons. It is also broadly consistent with new measurements of the spreading of energy near the entry surface discussed later. The conversion efficiency from laser energy to electron energy was defined using the local intensity and a fit to a compilation of experimental data on conversion to electron energy at different intensities.

With this model 100J of laser energy was converted to 27 J of electrons injected into a 100 μm thick target. Tracer particles showed the electron trajectories as illustrated in figure 5 on a map of magnetic field strength. The example is for particles injected along the axis at 10 μm radius at times near the peak of the laser pulse. The complexity of the refluxing transport is clearly seen. The computation was continued for 6 ps well beyond the end of the 1ps laser pulse, in order to find the temporal peak of the temperature in each cell. The results for the radial profile of peak temperature at the rear surface are in remarkably good agreement with the XUV imaging measurements as shown in figure 2. The wide pediment in the XUV deduced temperature profile which is not seen in the $K\alpha$ data (figure4), could be due to a rear surface current or to slower heat conduction by electrons of energy too low to excite $K\alpha$. LSP shows a similar pediment in the bulk of the target and the possibility that this is due to a slower conduction wave is being investigated.

Despite the good agreement in the rear surface temperature profile, this is not yet a benchmarked model because the injected electron characteristics were obtained from a heuristic rather than an ab-

initio model. An ab-initio approach would use 3D PIC modeling to describe the interaction of the measured vacuum intensity pattern of the focused laser radiation with a measured (or hydro-code calculated) pre-formed plasma due to ASE and leakage pulses.

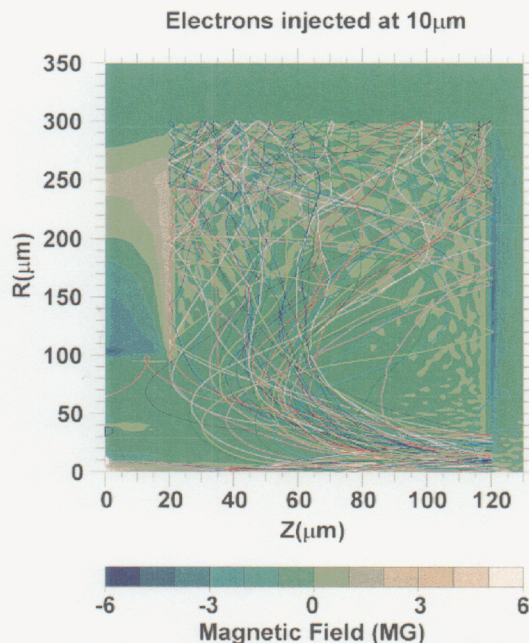


Figure 5 LSP model of 100 μm Al showing trajectories of electrons injected perpendicular to the left surface at $r=10\mu\text{m}$ near the temporal peak of the pulse. The background contours show the magnetic field.

Such modeling would show relativistic self-focusing and filamentation and electron acceleration in the underdense and critical density plasma. For one or two decades of density above critical density where the hot electron to background plasma density ratio is largest and electron transport instabilities most important, it could also track the Weibel-like filamentation and two stream unstable axial bunching of the electron flow, the associated collision-less energy transfer from the electron beam to the background plasma and the transverse surface waves. These phenomena would result in injection of electrons into the high density target in a specific angular pattern and energy spectrum. In our work this PIC modeling is being developed but is not yet mature enough to produce results, which would enable a true benchmarking of an integrated model.

In recent experiments we have extended the $K\alpha$ imaging technique to study transport in a homogeneous target with a 50:50 by weight mixture of Al and Cu. The laser was incident 50 μm from the

edge of the target and the 39° off perpendicular view angle shows both the emission from the irradiated front surface and a side view of the emission inside the target. This revealed a strong spreading of transport over a 50 μm radius near the entry surface and rapid axial attenuation in about 20 μm , as seen in figure 6. The observations lend support to the heuristic model of the electron source, which assumes significant divergence in the lower energy component of the electrons. These electrons arguably have a range of the order of the observed emission radius.

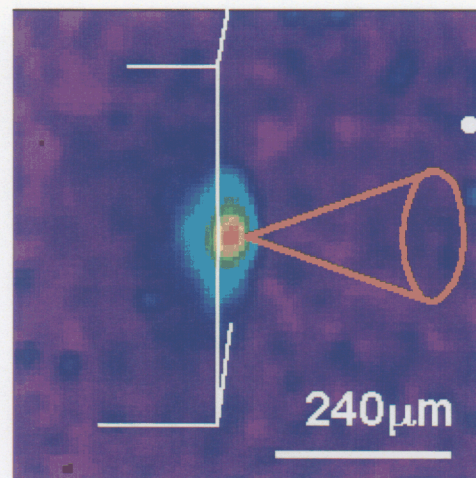


Figure 6 $K\alpha$ image from 39° off perpendicular view of Cu doped Al target irradiated 50 μm from its edge

Study of transport via hollow Au cones of interest for fast ignition, was also begun with an experiment in which the cone was attached to a similar Al/Cu target. The image in figure 7 showed similar lateral spreading to that without the cone, (note the obscuration of the view of the emission by the tip of the cone) but with an order of magnitude less intensity, consistent with the cone stopping most the lower energy electrons because its mass per unit area matched that of the Al in the previously noted 50 μm radial range.

The concentration of electron flux at the tip of the cone was measured by imaging a cone with a 2 μm thick Cu coating on its outside surface as shown in Figure 8.

Modeling and further analysis of these new data will be discussed in future work.

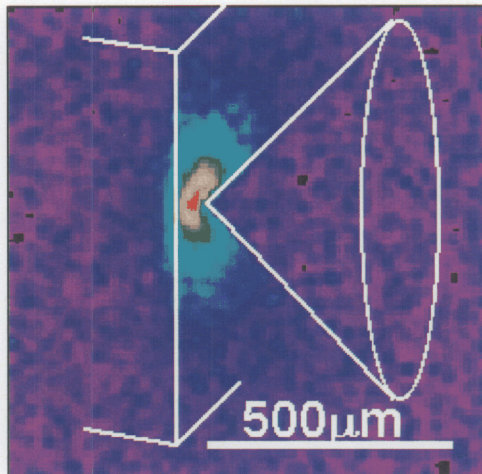


Figure 7 $K\alpha$ image as in figure 6 but with irradiation via a hollow Au cone.

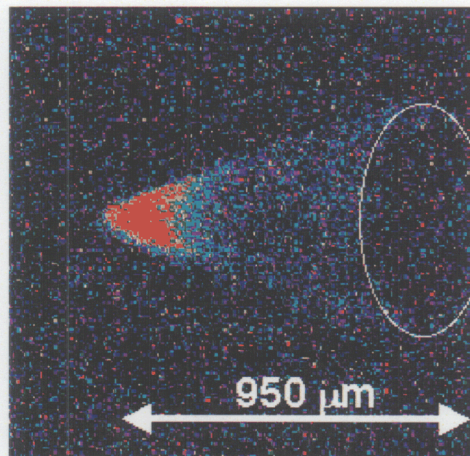


Figure 8 $K\alpha$ image of an Au hollow cone coated outside with $2\mu\text{m}$ Cu irradiated at its inside tip.

Conclusions

A significant step towards a predictive capability for electron transport and isochoric heating has been made through demonstrated good agreement between detailed experimental measurements of transport and heating in Al targets and hybrid PIC modeling with injected electron characteristics from an experiment based heuristic model. This is potentially valuable for the design of any application of intense short pulse lasers and particularly important for fast ignition where major scale up from current experiments is needed. There remains a need for an ab-initio model of the electron source and effort is currently being directed to PIC modeling to

accomplish this. New experiments on transport in homogeneous Cu doped Al and via Au cones used in fast ignition targets, show interesting information, qualitatively consistent with the heuristic model we developed to define the electron source. These new data will be further analyzed and modeled in future work.

Acknowledgments

Work performed under the auspices of the U.S. Department of Energy by the Lawrence Livermore National Laboratory under Contract No. W-7405-ENG-48.

References

- [¹] J A Koch et al. PRE 65016510 (2001). M H Key et al. Inertial Fusion Sciences and applications 2001. P357. M. H. Key et al. Proc. 19th IAEA Fusion Energy Conference, Lyon France Oct. (2002), R Stephens et al PRE (submitted).
- [²] D. R. Welch, D. V. Rose, B. V. Oliver, and R. E. Clark, Nucl. Inst. Meth. Phys. Res. A **242**, 134 (2001).
- ³ H.M. Milchberg, et al., Phys. Rev. Lett. **62** 2364 (1988).
- ⁴ see R Town et al ibid